

## Evanescent-Vacuum-Enhanced Photon-Exciton Coupling and Fluorescence Collection

Juanjuan Ren,<sup>1</sup> Ying Gu,<sup>1,2,\*</sup> Dongxing Zhao,<sup>1</sup> Fan Zhang,<sup>1</sup> Tiancai Zhang,<sup>2,3</sup> and Qihuang Gong<sup>1,2</sup>

<sup>1</sup>*State Key Laboratory for Mesoscopic Physics, Collaborative Innovation Center of Quantum Matter, Department of Physics, Peking University, Beijing 100871, China*

<sup>2</sup>*Collaborative Innovation Center of Extreme Optics, Shanxi University, Taiyuan, Shanxi 030006, China*

<sup>3</sup>*State Key Laboratory of Quantum Optics and Quantum Optics Devices, Institute of Opto-Electronics, Shanxi University, Taiyuan 030006, China*

(Received 18 August 2016; published 17 February 2017)

An evanescent optical mode existing in various nanophotonic structures always acts as a cavity mode rather than an electromagnetic vacuum in the study of cavity quantum electrodynamics (CQED). Here we show that taking the evanescent mode as an electromagnetic vacuum in which the nanocavity is located is possible through the optical mode design. The proposed evanescent vacuum enables us to enhance both the reversible photon-exciton interaction and fluorescence collection. By embedding the custom-designed plasmon nanocavity into the evanescent vacuum provided by a metallic or dielectric nanowire, the photon-exciton coupling coefficient can achieve 4.2 times that in vacuum due to the exponential decay of the evanescent wave, and spontaneously emitted photons with Rabi splitting can be guided by an evanescent wave with a collection efficiency of 47% at most. Electromagnetic vacuum engineering at subwavelength scale holds promise for controlling the light-matter interaction in quantum optics, CQED, and on-chip quantum information.

DOI: [10.1103/PhysRevLett.118.073604](https://doi.org/10.1103/PhysRevLett.118.073604)

Requirements for handling on-chip quantum information and building scalable quantum networks are prompting the development of nanostructure-based cavity quantum electrodynamics (CQED) characterized as strong light confinement [1–6]. Various optical modes arise in nanophotonic structures [2–5], among which plasmon nanostructures with an ultrasmall optical mode volume enable both reversible and irreversible light-matter interactions to be enhanced considerably [6–9]. Nevertheless, because of large intrinsic losses in metal, the strict strong-coupling regime, defined by the condition  $g_0 \gg \kappa, \gamma$  [1,10,11], is difficult to achieve; here  $g_0$ ,  $\kappa$ , and  $\gamma$  are the coupling coefficient of a single emitter, the cavity loss, and the decay rate of the quantum emitter (QE), respectively. In the plasmon-QE systems, by increasing the total number  $N$  of the emitters, the coupling coefficient  $g$  ( $=\sqrt{N}g_0$ ) is enhanced sufficiently to overcome cavity losses; hence, vacuum Rabi splitting of the fluorescence spectra and anticrossing among the energy levels have been observed experimentally [12–16]. However, although several theoretical studies have predicted a strong coupling regime between single QE and individual plasmon structure [17,18], this reversible interaction has rarely been realized experimentally [19].

Electromagnetic vacuum engineering plays a fundamental role in controlling light-matter interaction in quantum optics, CQED, and quantum information devices. The evanescent optical modes have ubiquitous presence in various nanowires, metallic nanofilms, and other nanostructures [20–23]. In previous studies [4,8,24], these modes are taken as cavity modes rather than providing

the electromagnetic vacuum environment that the cavity resides in. For combined plasmon nanostructures, the situation is nevertheless more complicated owing to the coupling or hybridization of multiple optical modes. When the interaction between the QE and optical modes is very weak, i.e., in the weak coupling regime, all optical modes can be viewed as constituting an electromagnetic background, so it is not necessary to distinguish cavity and background [25–27]. However, in the strong coupling regime, one should clarify the situation whether the modes are decoupled or hybridized [28]. For the decoupled situation, if the coupling coefficient between the QE and specific optical mode is greatly larger than that between the QE and other optical modes, then these modes can be looked as the electromagnetic background or vacuum.

In this Letter, by carefully designing the optical modes of the gap structure composed of the Ag nanorod (AgNR) and the nanowire [Fig. 1(a)], we can identify the dipolar mode of the AgNR as the nanocavity and the evanescent mode of the nanowire as electromagnetic vacuum, forming a nano-CQED system in evanescent vacuum (EV). The design is simple but sufficient to present an instance where the two optical modes decouple, in contrast to the instance of mode hybridization, where the entire structure of AgNR and nanowire should be viewed as a cavity [31–35]. Whereas the strong coupling has been studied extensively [12–19], exploiting the plasmon-exciton interaction in the strong coupling regime within an evanescent electromagnetic background has never been reported. Not limited to within present plasmon nanostructures, the idea of electromagnetic vacuum engineering can be extended to other

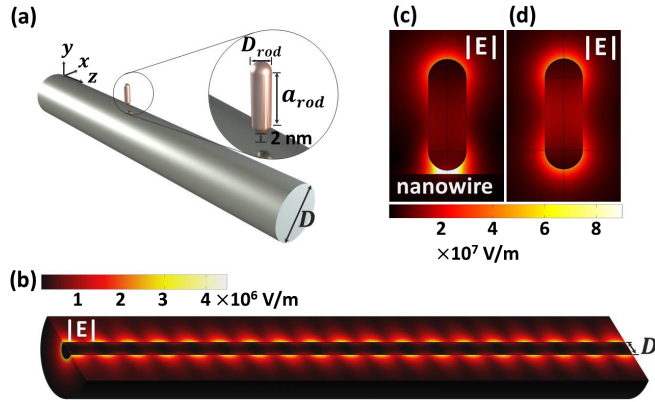


FIG. 1. Nano-CQED system embedded in EV. (a) Schematic diagram of AgNR nanocavity near the nanowire. (b) Evanescent wave of Ag nanowire. At  $\lambda = 780$  nm, the propagation constant  $k_z/k_0 = 1.747$ , which is consistent with the wavelength of evanescent wave of 447 nm. (c),(d) Electric field distributions of single excitation of the same size AgNR with and without a nanowire. With a Ag nanowire, the resonant length of the AgNR with  $D_{rod} = 20$  nm is  $a_{rod} = 38.6$  nm. While without a nanowire, the resonant wavelength is 670.7 nm.

custom-designed combined nanostructures with multiple optical modes.

By placing a resonant plasmon nanocavity into the EV provided by the dielectric or metallic nanowire [Fig. 1(a)], we theoretically demonstrate the enhanced reversible interaction between the single exciton and individual nanocavity. Originating from the exponential decay of the evanescent wave, the coupling coefficient is several times larger than that without a nanowire. Simultaneously, the spontaneously emitted photons with Rabi splitting can be collected with the efficiency of 12%–47% and guided by the evanescent wave of nanowires. The custom-tailoring vacuum can enhance both the plasmon-exciton coupling and fluorescence collection efficiency. Thus it raises the possibility for experimental observation of strong coupling between a single QE and individual plasmon structures. CQED in subwavelength-confined quantum vacuum holds promise for exploring fundamental physics and the applications related to on-chip quantum information and scalable quantum networks.

The mechanism to enhance the coupling coefficient via EV is described as follows. The coupling coefficient governing the interaction between the resonant AgNR and QE is defined as  $g_0 = [(\vec{\mu} \cdot \vec{E})/\hbar]$ , where  $\vec{\mu}$  denotes the transition dipole moment and  $\vec{E}$  is the field corresponding to a single excitation of the AgNR. In homogeneous vacuum, localized surface plasmons of the AgNR can be excited due to the collective oscillation of free electrons [36,37] [Fig. 1(d)]. While putting the AgNR in the EV provided by the nanowire [Fig. 1(b)], its localized surface plasmon can also be excited [Fig. 1(c)], where the field at the nanogap gets stronger than that at another end as the evanescent wave undergoes exponential decay. Naturally,

when the electromagnetic energy is normalized to a single excitation under the EV,  $g_0$  at the nanogap becomes larger than that in vacuum [Fig. 2(a)].

The specific nano-CQED system in the EV is shown in Fig. 1(a), where the AgNR with diameter  $D_{rod}$  and resonance length  $a_{rod}$  is vertically located in the vicinity of a nanowire, dielectric or metallic. The evanescent mode of the nanowire is squeezed into one spatial dimension [Fig. 1(b)]. Here, the nanorod is too small to affect the evanescent mode of the nanowire; i.e., their optical modes are decoupled; specifically, regardless of whether or not the AgNR is present, the propagation constant  $k_z$  is not changed. In the evanescent wave of the nanowire, the longitudinal mode of the AgNR can be excited. Therefore, the AgNR can be regarded as a nanocavity embedded in the subwavelength-confined electromagnetic vacuum. Alternatively, if the length of nanorod is comparable with the diameter of the nanowire, mode hybridization [31–35] between them can occur. In the following, single-mode nanowires enable us to collect fluorescence with high efficiency along one dimension. Choosing a dielectric nanowire reduces considerably the losses involved in guiding photons; in contrast, metallic nanowire with AgNR enhances significantly the photon-exciton coupling at the nanogap due to supporting gap surface plasmons [38–41].

The distance between the nanorod and nanowire is  $d = 2$  nm and the wavelength of light is  $\lambda = 780$  nm. The dielectric constant of metals is taken from the experimental data [42]. A dielectric nanowire of diameter 260 nm and permittivity  $\epsilon_{fiber} = 8.0$  is embedded in a medium of permittivity  $\epsilon_b = 2.13$ . It has single mode  $HE_{11}$  with  $k_z/k_0 = 2.138$  and penetration length of 79.5 nm [21]. For a metallic nanowire of diameter 120 nm, the propagation constant is  $\text{Re}(k_z/k_0) = 1.747$  and the penetration length is 129 nm [43]. Generally, the resonance wavelength of the AgNR in homogeneous vacuum is less than that in the EV. To calculate  $g_0$ ,  $\kappa$ , and  $\gamma$ , 3D finite-element simulations were performed using COMSOL Multiphysics software [27,28,44].

Under the dipole and rotating wave approximations, the Hamiltonian of the emitter-cavity system in an EV can be written as  $H = \hbar\omega_e\sigma^\dagger\sigma + \hbar\omega_c a^\dagger a + \hbar g_0(\sigma^\dagger a + \sigma a^\dagger)$ , where  $\sigma^\dagger$  and  $\sigma$  are the raising and lowering operators of the emitter, and  $a^\dagger$  and  $a$  are creation and annihilation operators of the longitudinal mode of AgNR. We let  $\omega_e$  and  $\omega_c$  denote the frequencies of the emitter and the AgNR nanocavity. The Hamiltonian has the same form as that in a traditional CQED system [45], but now  $g_0$  denotes the coupling coefficient between the QE and longitudinal mode of AgNR in the EV. Note that the evanescent mode only provides a thermal reservoir in which the nano-CQED system resides. The dynamics of the CQED system is governed by the master equation  $\dot{\rho} = -(i/\hbar)[H, \rho] - (\gamma/2)(\sigma^\dagger\sigma\rho - \sigma\rho\sigma^\dagger + \text{H.c.}) - (\kappa/2)(a^\dagger a\rho - \rho a^\dagger a + \text{H.c.})$ . Two dissipative channels influence the evolution: the damping rate  $\kappa$  of the nanocavity to the thermal reservoir via Ohmic loss and the decay rate  $\gamma$  of the emitter to modes other than the AgNR nanocavity mode.  $\gamma = \gamma_{ev} + \gamma_{rad}$ , for

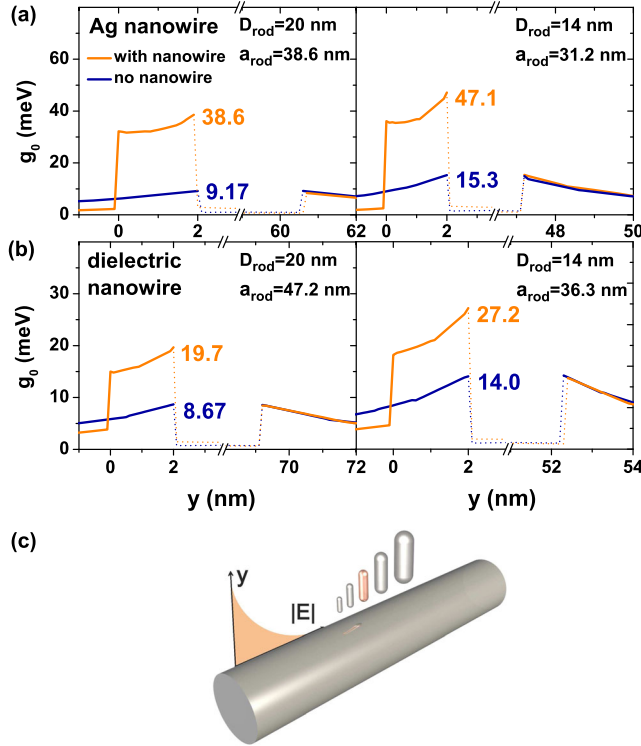


FIG. 2. Mechanism of enhancing the coupling coefficient via EV. (a),(b)  $g_0$  along the central axis of AgNR for a Ag nanowire and dielectric nanowire systems. (c) Schematic diagram of the AgNRs with variable size in the evanescent wave.

which  $\gamma_{ev}$  originates from the EV, whereas  $\gamma_{rad}$  describes how the system radiates to far field.

First the enhancement of  $g_0$  in the EV is demonstrated. The calculation and validity of  $g_0$  are presented in Ref. [28]. For both Ag and dielectric nanowire systems, the variation of  $g_0$  along the central axis for four AgNRs of various sizes is shown in Figs. 2(a) and 2(b). Here, the QE is  $y$ -axis orientated and its transition dipole moment is  $\mu = 0.2$  enm. Comparing the results with and without nanowires, the coupling coefficients at the nanogap were found to be 1.9–4.2 times of that without nanowires. Because the evanescent wave decays exponentially [Fig. 1(b) and Fig. 2(c)], the electromagnetic fields at the nanogap are more localized; for the homogeneous vacuum, the electric field distribution of resonant AgNR is symmetric [Fig. 1(d)] [37]. Thus in an EV, the energy redistribution of single-photon excitation leads to the enhancement of coupling coefficients at the nanogap.

Comparing nanorods with same diameter  $D_{rod}$  near different nanowires [Figs. 2(a) and 2(b)], there is only a slight difference in the resonance length  $a_{rod}$ , but the enhancement (4.21,3.08) of  $g_0$  near the Ag nanowire is larger than that (2.27,1.94) near the dielectric nanowire. The main reason is the existence of a gap surface plasmon [38–41], where the charges at the end of nanorod induce the gathering of charges with opposite sign at the surface of metallic nanowire, leading to more enhanced field.

Therefore, to obtain larger enhancement of  $g_0$ , plasmon nanostructures are preferred.

To further enhance the coupling coefficients  $g_0$ , we increased the size of the AgNR. For both metallic and dielectric nanowires, the resonance length  $a_{rod}$  becomes longer with increasing diameter  $D_{rod}$  (see Fig. 2 or Ref. [28]). The enhancement of  $g_0$  continues because within the penetration length of the evanescent wave, the longer nanorod can receive more electric field attenuation [Fig. 2(c)]. Moreover, with increasing nanorod size, the coupling coefficients decrease because the optical mode volume increases.

Then, we describe the reversible interaction between the surface plasmon and the exciton in the EV. With the present emitter-nanocavity systems,  $\kappa$  is generally in the range 30–120 meV, and with increasing dipole moment  $\mu$ ,  $g_0$  and  $\gamma$  vary from several  $\mu$ eV to several tens meV. The calculation and validity of  $\kappa$  and  $\gamma$  are given in Ref. [28]. Consider a specific AgNR resonator with  $D_{rod} = 14$  nm and  $a_{rod} = 31.2$  nm near single-mode Ag nanowire. The emitter is at the center of nanogap with  $g_0^{mid}$ . Its transition frequency is exactly resonant with cavity mode of the AgNR. Initially, the emitter is excited and there is no photon in the nanocavity.

With the above parameters, the cavity loss is constant with  $\kappa = 67$  meV, and  $g_0^{mid}$  and  $\gamma$  are, respectively, linearly and quadratically proportional to the dipole moment [Fig. 3(a)]. We use Python toolbox to calculate the expectation values  $\rho_{ee}$  and  $\rho_{nn}$  of excitons and cavity photons and fluorescence spectra [28]. When  $\mu > 0.15$  enm, the QE and cavity photons begin exchanging energy periodically, accompanied by small Rabi splitting in the fluorescence spectra; when  $\mu > 0.5$  enm, an obvious reversible interaction between them occurs [insets in Fig. 3(a)]. And, with increasing  $\mu$ , the splitting becomes larger. The positions of these splitting peaks are roughly at  $\pm g_0^{mid}$ , and the peak widths broaden with dependence  $(\kappa + \gamma)$ , in agreement with the predictions from dressed state analysis [46]. In real experiments, the dephasing rate originating from the environment should be considered. In room temperature, the dephasing rate of the atoms is generally less than 1 meV [47], so it can be ignored here. For the quantum dots or molecules, this value nevertheless can achieve from several to several tens of mega-electron-volts, which greatly broadens the linewidth of peaks, namely, to achieve strong coupling, a larger coupling coefficient is needed.

By careful COMSOL simulation [28], it is found that Ref. [19] has provided strong experimental support for our theory. With the parameters provided by Ref. [19], we first obtained the absorption spectrum of Au nanosphere with the resonance wavelength of  $\lambda = 660$  nm and linewidth of  $\kappa = 100.1$  meV, which are in agreement with the experimental results of  $\lambda = 660 \pm 10$  nm and  $\kappa = 122$  meV. The single peak in the absorption spectrum implies that we can use the viewpoint of EV to calculate  $g_0$ . Then, we got the result of  $g_0^{mid} = 47.84$  meV, in agreement with the experiment result of  $g_0^{mid} = 45$  meV in Ref. [19]. Using the parameters of  $\gamma = 85$  meV measured at room temperature,

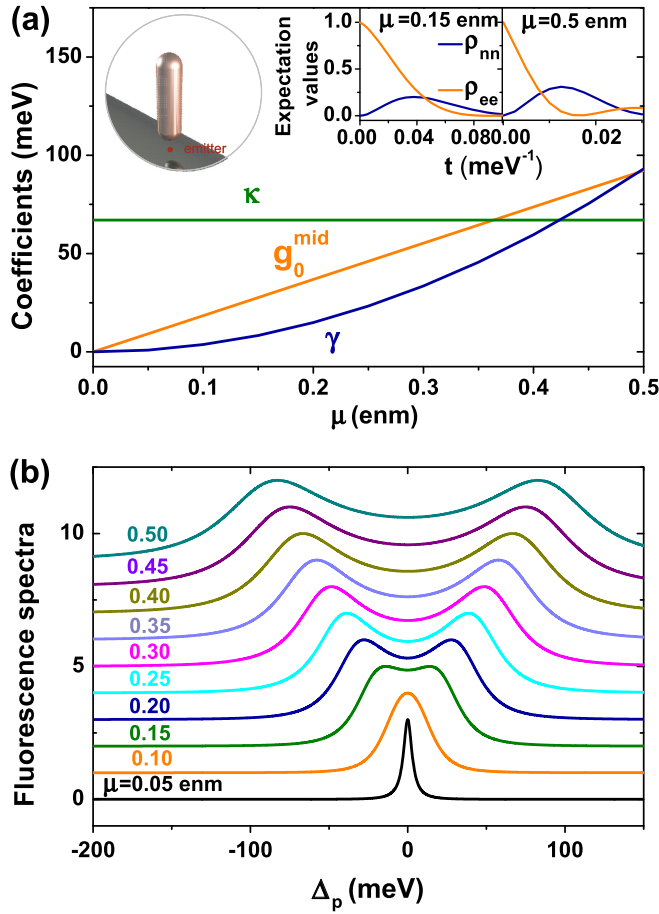


FIG. 3. Reversible interaction in EV. (a) Coupling coefficients  $g_0^{\text{mid}}$  and decay rates  $\gamma$  of a single emitter at the center of the nanoscale gap, and decay rates  $\kappa$  of a AgNR nanocavity in the Ag nanowire system. Insets in (a) show the expectation values of  $\rho_{nn}$  and  $\rho_{ee}$  for  $\mu = 0.15$  enm and  $0.5$  enm. (b) Fluorescence spectra for different dipole moments as a function of the detuning  $\Delta_p = \omega - \omega_e$ .

and  $g$  for ten QEs,  $\kappa$  calculated by the simulations, the resonance fluorescence spectrum with Rabi splitting are obtained, whose position and linewidth of peaks are consistent with Ref. [19].

Next, we discuss the fluorescence collection through the EV. A weak fluorescence signal and large divergence angle hindered the experimental measurement in the photonic nanostructures. In the irreversible interaction, one ingenious and successful solution is utilizing the evanescent wave provided by the nanofiber, metallic nanowire, and gap surface plasmon nanostructures to collect the enhanced spontaneously emitted photons [4,5,8,9,24,27,48]. Here, by taking the advantage of an evanescent wave, the nanowire can both collect and guide the emitted photons. The total decay rate of emission photons is  $\gamma_t = \gamma + \gamma_{\text{nr}} = \gamma_{\text{ev}} + \gamma_{\text{rad}} + \gamma_{\text{nr}}$ , where  $\gamma_{\text{nr}}$  is the nonradiative decay rate to the AgNR. For the Ag nanowire system, besides the Ohmic loss of AgNR itself,  $\gamma_{\text{nr}}$  also includes the absorption of both the images of AgNR and the emitter in the nanowire [27]. The nanowire collects the guiding part  $\gamma_{\text{ev}}$  into the

TABLE I. High fluorescence collection efficiency through EV. (a),(b) Collection efficiency for Ag and dielectric nanowires.

$(D_{\text{rod}}, a_{\text{rod}})$ (nm)	Collection efficiency
(a) Ag nanowire	
10, 24.5	33.0%
14, 31.2	41.9%
20, 38.6	47.0%
(b) Dielectric nanowire	
10, 27.4	12.2%
14, 36.3	18.1%
20, 47.2	22.3%

evanescent wave, so the channelling efficiency of fluorescence is defined as  $\eta = (\gamma_{\text{ev}}/\gamma_t)$ .

With the emitter still at the nanogap,  $\eta$  for metallic and dielectric nanowires can achieve 33%–47% and 12%–22% respectively (see Table I). The results with a dielectric nanowire are roughly in agreement with the channelling efficiency of 22.0( $\pm$ 4.8)% obtained by putting single quantum dots close to the optical nanofiber [4]. With increasing the size of AgNR,  $\eta$  increases for both nanowires. When the longitudinal mode of a longer AgNR in an evanescent wave is excited, more localized fields are gathered at the nanogap, resulting in the higher channelling efficiency. The fluorescence in the present nano-CQED system can be efficiently collected via the evanescent wave. And these propagating photons can be directly used in on-chip quantum devices.

We compared the results from metallic and dielectric nanowires (Table I) combined with a AgNR that is almost the same except that the corresponding resonance length is slightly changed. The channelling efficiency  $\eta$  in the Ag nanowire system was found to be larger than that in the dielectric nanowire system. Because the gap plasmon [38–41] with a more localized electromagnetic field at the nanoscale gap causes a larger  $\eta$ . For a Ag nanowire system, although a larger  $\eta$  is obtained, the propagation length of the emitted photons is only over ten micrometers, which to some extent limits its applications in on-chip photonics. Thus, if only the channeling capability of the fluorescence is of concern, low-loss dielectric nanowires are preferable.

Finally, with currently available nanotechnologies, individual nanowire [4,20,49] and metallic nanoparticles [50] have been controllably fabricated. Using the techniques that accurately control the gap in nanoparticle-coupled nanofilm structures [19,26,40,51], a nanoscale gap between the AgNR and nanowire can in principle be formed. Aligning terrylene molecules in a spin-coated ultrathin crystalline film of *p*-terphenyl has been realized, so inserting a single upright emitter in the nanoscale gap is very promising [52]. The excited state of the emitter can be prepared in two ways. One is via total internal reflection of the *p*-polarized incident light through a microscope objective [53]. The other way is exciting the emitter by the

longitudinal mode of a AgNR in the evanescent wave of a nanowire. The evanescent wave can be excited via near-field overlapping technique using an optical nanofiber taper [54]. Thus using present techniques, experimentally realizing our CQED protocol is possible.

In summary, by proposing the concept of the EV, we have theoretically demonstrated the enhanced reversible interaction in a plasmon nanocavity embedded in the EV. Simultaneously, using the specific property of the evanescent wave whereby the optical mode is squeezed into one spatial dimension, the emitted photons with the collection efficiency of 12%–47% can be guided into the nanowire. Enhanced interaction and high collection efficiency in the EV enables the experimental observation of a single emitter coupled to a plasmon CQED system. Hence, by engineering the vacuum at subwavelength scale, we have developed a novel quantum interface for studying the CQED, where typical phenomena in traditional CQED [11,55], such as reversible interaction, entanglement, and state manipulation, are expected to be realized. Apart from its fundamental interest, the CQED in subwavelength-confined quantum vacuum should have an impact on on-chip quantum information technologies and scalable quantum network applications.

This work was supported by the National Key Basic Research Program under Grant No. 2013CB328700, and by the National Natural Science Foundation of China under Grants No. 11525414, No. 11374025, and No. 91221304.

\*ygu@pku.edu.cn

- [1] K. J. Vahala, Optical microcavities, *Nature (London)* **424**, 839 (2003).
- [2] Y. Akahane, T. Asano, B.-S. Song, and S. Noda, High-Q photonic nanocavity in a two-dimensional photonic crystal, *Nature (London)* **425**, 944 (2003).
- [3] T. Yoshie, A. Scherer, J. Hendrickson, G. Khitrova, H. M. Gibbs, G. Rupper, C. Ell, O. B. Shchekin, and D. G. Deppe, Vacuum Rabi splitting with a single quantum dot in a photonic crystal nanocavity, *Nature (London)* **432**, 200 (2004).
- [4] R. Yalla, F. L. Kien, M. Morinaga, and K. Hakuta, Efficient Channeling of Fluorescence Photons from Single Quantum Dots into Guided Modes of Optical Nanofiber, *Phys. Rev. Lett.* **109**, 063602 (2012).
- [5] R. Yalla, M. Sadgrove, K. P. Nayak, and K. Hakuta, Cavity Quantum Electrodynamics on a Nanofiber Using a Composite Photonic Crystal Cavity, *Phys. Rev. Lett.* **113**, 143601 (2014).
- [6] M. S. Tame, K. R. McEnery, S. K. Özdemir, J. Lee, S. A. Maier, and M. S. Kim, Quantum plasmonics, *Nat. Phys.* **9**, 329 (2013).
- [7] Z. Jacob and V. M. Shalaev, Plasmonics goes quantum, *Science* **334**, 463 (2011).
- [8] A. V. Akimov, A. Mukherjee, C. L. Yu, D. E. Chang, A. S. Zibrov, P. R. Hemmer, H. Park, and M. D. Lukin, Generation of single optical plasmons in metallic nanowires coupled to quantum dots, *Nature (London)* **450**, 402 (2007).
- [9] D. E. Chang, A. S. Sørensen, P. R. Hemmer, and M. D. Lukin, Quantum Optics with Surface Plasmons, *Phys. Rev. Lett.* **97**, 053002 (2006).
- [10] O. Benson, Assembly of hybrid photonic architectures from nanophotonic constituents, *Nature (London)* **480**, 193 (2011).
- [11] H. J. Kimble, The quantum internet, *Nature (London)* **453**, 1023 (2008).
- [12] J. Bellessa, C. Bonnard, and J. C. Pleniet, Strong Coupling between Surface Plasmons and Excitons in an Organic Semiconductor, *Phys. Rev. Lett.* **93**, 036404 (2004).
- [13] T. K. Hakala, J. J. Toppari, A. Kuzyk, M. Pettersson, H. Tikkanen, H. Kunttu, and P. Törmä, Vacuum Rabi Splitting and Strong-Coupling Dynamics for Surface-Plasmon Polaritons and Rhodamine 6G Molecules, *Phys. Rev. Lett.* **103**, 053602 (2009).
- [14] D. E. Gómez, K. C. Vernon, P. Mulvaney, and T. J. Davis, Surface plasmon mediated strong exciton-photon coupling in semiconductor nanocrystals, *Nano Lett.* **10**, 274 (2010).
- [15] A. E. Schlather, N. Large, A. S. Urban, P. Nordlander, and N. J. Halas, Near-field mediated plexcitonic coupling and giant Rabi splitting in individual metallic dimers, *Nano Lett.* **13**, 3281 (2013).
- [16] G. Zengin, M. Wersäll, S. Nilsson, T. J. Antosiewicz, M. Käll, and T. Shegai, Realizing Strong Light-Matter Interactions between Single-Nanoparticle Plasmons and Molecular Excitons at Ambient Conditions, *Phys. Rev. Lett.* **114**, 157401 (2015).
- [17] E. Waks and D. Sridharan, Cavity QED treatment of interactions between a metal nanoparticle and a dipole emitter, *Phys. Rev. A* **82**, 043845 (2010).
- [18] S. Savasta, R. Saija, Alessandro Ridolfo, O. D. Stefano, P. Denti, and F. Borghese, Nanopolaritons: vacuum Rabi splitting with a single quantum dot in the center of a dimer nanoantenna, *ACS Nano* **4**, 6369 (2010).
- [19] R. Chikkaraddy, B. d. Nijs, F. Benz, S. J. Barrow, O. A. Scherman, E. Rosta, A. Demetriadou, P. Fox, O. Hess, and J. J. Baumberg, Single-molecule strong coupling at room temperature in plasmonic nanocavities, *Nature (London)* **535**, 127 (2016).
- [20] L. Tong, R. R. Gattass, J. B. Ashcom, S. He, J. Lou, M. Shen, I. Maxwell, and E. Mazur, Subwavelength-diameter silica wires for low-loss optical wave guiding, *Nature (London)* **426**, 816 (2003).
- [21] L. Tong, J. Lou, and E. Mazur, Single-mode guiding properties of subwavelength-diameter silica and silicon wire waveguides, *Opt. Express* **12**, 1025 (2004).
- [22] B.-Q. Sun, Y. Gu, X.-Y. Hu, and Q.-H. Gong, A trade-off between propagation length and light confinement in cylindrical metal-dielectric waveguides, *Chin. Phys. Lett.* **28**, 057303 (2011).
- [23] A. V. Zayats, I. I. Smolyaninov, and A. A. Maradudin, Nano-optics of surface plasmon polaritons, *Phys. Rep.* **408**, 131 (2005).
- [24] S. Kato and T. Aoki, Strong Coupling between a Trapped Single Atom and an All-Fiber Cavity, *Phys. Rev. Lett.* **115**, 093603 (2015).
- [25] K. J. Russell, T.-L. Liu, S. Cui, and E. L. Hu, Large spontaneous emission enhancement in plasmonic nanocavities, *Nat. Photonics* **6**, 459 (2012).

- [26] G. M. Akselrod, C. Argyropoulos, T. B. Hoang, C. Ciraci, C. Fang, J. Huang, D. R. Smith, and M. H. Mikkelsen, Probing the mechanisms of large Purcell enhancement in plasmonic nanoantennas, *Nat. Photonics* **8**, 835 (2014).
- [27] H. Lian, Y. Gu, J. Ren, F. Zhang, L. Wang, and Q. Gong, Efficient Single Photon Emission and Collection Based on Excitation of Gap Surface Plasmons, *Phys. Rev. Lett.* **114**, 193002 (2015).
- [28] See Supplemental Material at <http://link.aps.org/supplemental/10.1103/PhysRevLett.118.073604> for dispersion of nanowires' evanescent mode, longitudinal mode of AgNR in evanescent vacuum, mode coupling between the AgNR and the nanowire, validity of computation for coupling coefficients, decay rate of the emitter and the AgNR cavity loss, computation relative to reversible interactions, and experimental support, which includes Refs. [29,30].
- [29] K. Slowik, R. Filter, J. Straubel, F. Lederer, and C. Rockstuhl, Strong coupling of optical nanoantennas and atomic systems, *Phys. Rev. B* **88**, 195414 (2013).
- [30] J. R. Johansson, P. D. Nation, and F. Nori, QuTiP 2: A Python framework for the dynamics of open quantum systems, *Nano Lett.* **14**, 1234 (2013).
- [31] P. Wang, Y. Wang, Z. Yang, X. Guo, X. Lin, X.-C. Yu, Y.-F. Xiao, W. Fang, L. Zhang, G. Lu, Q. Gong, and L. Tong, Single-band 2-nm-line-width plasmon resonance in a strongly coupled Au nanorod, *Nano Lett.* **15**, 7581 (2015).
- [32] C. Tserkezis, R. Esteban, D. O. Sigle, J. Mertens, L. O. Herrmann, J. J. Baumberg, and J. Aizpurua, Hybridization of plasmonic antenna and cavity modes: Extreme optics of nanoparticle-on-mirror nanogaps, *Phys. Rev. A* **92**, 053811 (2015).
- [33] A. Trügler and U. Hohenester, Strong coupling between a metallic nanoparticle and a single molecule, *Phys. Rev. B* **77**, 115403 (2008).
- [34] A. Gonzalez-Tudela, F. J. Rodríguez, L. Quiroga, and C. Tejedor, Dissipative dynamics of a solid-state qubit coupled to surface plasmons: From non-Markov to Markov regimes, *Phys. Rev. B* **82**, 115334 (2010).
- [35] C. Van Vlack, P. T. Kristensen, and S. Hughes, Spontaneous emission spectra and quantum light-matter interactions from a strongly coupled quantum dot metal-nanoparticle system, *Phys. Rev. B* **85**, 075303 (2012).
- [36] H. Raether, *Surface Plasmons on Smooth and Rough Surfaces and on Gratings* (Springer-Verlag Press, Berlin, 1986).
- [37] K. L. Kelly, E. Coronado, L. L. Zhao, and G. C. Schatz, The optical properties of metal nanoparticles: the influence of size, shape, and dielectric environment, *J. Phys. Chem. B* **107**, 668 (2003).
- [38] F. Le, N. Z. Lwin, J. M. Steele, M. Käll, N. J. Halas, and P. Nordlander, Plasmons in the metallic nanoparticle-film system as a tunable impurity problem, *Nano Lett.* **5**, 2009 (2005).
- [39] J. J. Mock, R. T. Hill, A. Degiron, S. Zauscher, A. Chilkoti, and D. R. Smith, Distance-dependent plasmon resonant coupling between a gold nanoparticle and gold film, *Nano Lett.* **8**, 2245 (2008).
- [40] J. B. Lassiter, F. McGuire, J. J. Mock, C. Ciraci, R. T. Hill, B. J. Wiley, A. Chilkoti, and D. R. Smith, Plasmonic waveguide modes of film-coupled metallic nanocubes, *Nano Lett.* **13**, 5866 (2013).
- [41] G. Lévêque and O. J. F. Martin, Optical interactions in a plasmonic particle coupled to a metallic film, *Opt. Express* **14**, 9971 (2006).
- [42] P. B. Johnson and R. W. Christy, Optical constants of noble metals, *Phys. Rev. B* **6**, 4370 (1972).
- [43] P.-F. Yang, Y. Gu, and Q.-H. Gong, Surface plasmon polariton and mode transformation in a nanoscale lossy metallic cylindrical cable, *Chin. Phys. B* **17**, 3880 (2008).
- [44] X. Shan, I. Díez-Pérez, L. Wang, P. Wiktor, Y. Gu, L. Zhang, W. Wang, J. Lu, S. Wang, Q. Gong, J. Li, and N. Tao, Imaging the electrocatalytic activity of single nanoparticles, *Nat. Nanotechnol.* **7**, 668 (2012).
- [45] H. J. Kimble, Strong interactions of single atoms and photons in cavity QED, *Phys. Scr.* **T76**, 127 (1998).
- [46] C. Cohen-Tannoudji and S. Reynaud, Dressed-atom description of resonance fluorescence and absorption spectra of a multi-level atom in an intense laser beam, *J. Phys. B* **10**, 345 (1977).
- [47] S. Kuhr, W. Alt, D. Schrader, I. Dotsenko, Y. Miroshnychenko, A. Rauschenbeutel, and D. Meschede, Analysis of dephasing mechanisms in a standing-wave dipole trap, *Phys. Rev. A* **72**, 023406 (2005).
- [48] A. Goban, C.-L. Hung, J. D. Hood, S.-P. Yu, J. A. Muniz, O. Painter, and H. J. Kimble, Superradiance for Atoms Trapped along a Photonic Crystal Waveguide, *Phys. Rev. Lett.* **115**, 063601 (2015).
- [49] H. Dittlacher, A. Hohenau, D. Wagner, U. Kreibig, M. Rogers, and F. Hofer, Silver Nanowires as Surface Plasmon Resonators, *Phys. Rev. Lett.* **95**, 257403 (2005).
- [50] B. J. Wiley, Y. Chen, J. M. McLellan, Y. Xiong, Z.-Y. Li, D. Ginger, and Y. Xia, Synthesis and optical properties of silver nanobars and nanorice, *Nano Lett.* **7**, 1032 (2007).
- [51] D. O. Sigle, J. T. Hugall, S. Ithurria, B. Dubertret, and J. J. Baumberg, Probing Confined Phonon Modes in Individual CdSe Nanoplatelets using Surface-Enhanced Raman Scattering, *Phys. Rev. Lett.* **113**, 087402 (2014).
- [52] R. J. Pfab, J. Zimmermann, C. Hettich, I. Gerhardt, A. Renn, and V. Sandoghdar, Aligned terrylene molecules in a spin-coated ultrathin crystalline film of *p*-terphenyl, *Chem. Phys. Lett.* **387**, 490 (2004).
- [53] K. G. Lee, X. W. Chen, H. Eghlidi, P. Kukura, R. Lettow, A. Renn, V. Sandoghdar, and S. Göttinger, A planar dielectric antenna for directional single-photon emission and near-unity collection efficiency, *Nat. Photonics* **5**, 166 (2011).
- [54] X. Guo, M. Qiu, J. Bao, B. J. Wiley, Q. Yang, X. Zhang, Y. Ma, H. Yu, and L. Tong, Direct coupling of plasmonic and photonic nanowires for hybrid nanophotonic components and circuits, *Nano Lett.* **9**, 4515 (2009).
- [55] H. Walther and B. T. H. Varcoe and B.-G. Englert, and T. Becker, Cavity quantum electrodynamics, *Rep. Prog. Phys.* **69**, 1325 (2006).